

# Preparation and heat-insulating property of the bio-inspired $\text{ZrO}_2$ fibers based on the silk template

Tianchi Wang<sup>a,b,\*</sup>, Song Kong<sup>a</sup>, Lijing Chang<sup>a</sup>, Chingping Wong<sup>b,\*\*</sup>

<sup>a</sup>*School of Materials Science and Engineering, Nanjing University of Science and Technology, Nanjing 210094, China*

<sup>b</sup>*School of Materials Science and Engineering, Georgia Institute of Technology, Atlanta, GA 30332, USA*

Received 26 March 2012; received in revised form 14 May 2012; accepted 23 May 2012

Available online 30 May 2012

## Abstract

Natural silk fibers were used as the template to prepare biomorphic  $\text{ZrO}_2$  fibers. Silk fibers were first immersed into a  $\text{Zr}(\text{NO}_3)_4$  solution and then sintered in air at high temperatures to produce the final  $\text{ZrO}_2$  fibers. Their microstructures, phases, synthesis process, infrared absorption spectra and thermal conductivity were analyzed. The results show that these synthesized fibers retained the morphologies of silk faithfully. These  $\text{ZrO}_2$  fibers also obtained the ability of absorbing infrared from the silk, so that they possessed better heat-insulating property than the traditional  $\text{ZrO}_2$  fibers.

© 2012 Elsevier Ltd and Techna Group S.r.l. All rights reserved.

**Keywords:** C. Thermal conductivity; D.  $\text{ZrO}_2$ ; Fibers; Silk

## 1. Introduction

In industry, zirconia ( $\text{ZrO}_2$ ) fiber is usually used as a heat insulator due to its good heat-insulating property. It has been made into the lining of various furnaces, heat-insulating layer in the spacecrafts and aircrafts, diaphragm in the fuel cells, insulating materials in the atomic energy reactors, etc. These days,  $\text{ZrO}_2$  fibers can be fabricated mainly by the precursor methods, such as the sol–gel method, the hybrid method, the immersion method, etc. [1–4]. Through these methods, fibrous precursor is obtained first by spinning the solution or collosol that contains zirconic ion. Then  $\text{ZrO}_2$  fibers are got by sintering the precursor in air or oxygen. It is obvious that the shapes of these  $\text{ZrO}_2$  fibers were completely artificially controlled.

Recently, ceramics mimicking the bio-structures of natural tissues have attracted increasing interest. In comparison to synthetic materials, natural materials such as bamboo, wood,

cotton, etc., possess intricate and graceful microstructures formed in a long-term evolution process. Researchers have used these bio-structures as templates to fabricate desired ceramics such as SiC, TiC,  $\text{Al}_2\text{O}_3$ ,  $\text{SnO}_2$ , etc., that retained the micro-morphologies of their original counterparts [5–12]. Results show that natural bio-structures can play an important role in obtaining new ceramic materials with excellent properties. These ceramics may be used for molecular screens, filters, catalyst support, thermal insulation materials, gas-sensing materials, electromagnetic shielding materials, far-infrared radiation materials, etc. The method of using the bio-templates provided a new and effective way to fabricate the materials with excellent properties.

Silk is an animal fiber made by silkworms. Fig. 1 shows the pod and the microstructure of the silk fibers. The main component of the silk is protein. A pile of silk has an excellent heat-insulating property, so it is often made into quilts. In the present work, we just select silk as a natural template to prepare biomorphic  $\text{ZrO}_2$  fibers. Their microstructures, phases, synthesis process, infrared absorption spectra and thermal conductivity were investigated. We hope this method could provide a new and handy way to fabricate  $\text{ZrO}_2$  fibers with an excellent heat-insulating property.

\*Corresponding author at: School of Materials Science and Engineering, Georgia Institute of Technology, Atlanta, GA 30332, USA.  
Tel.: +1 404 992 3747.

\*\*Corresponding author. Tel.: +1 404 894 8391.

E-mail addresses: [tianchiwang@yahoo.com.cn](mailto:tianchiwang@yahoo.com.cn) (T. Wang),  
[cp.wong@mse.gatech.edu](mailto:cp.wong@mse.gatech.edu) (C. Wong).

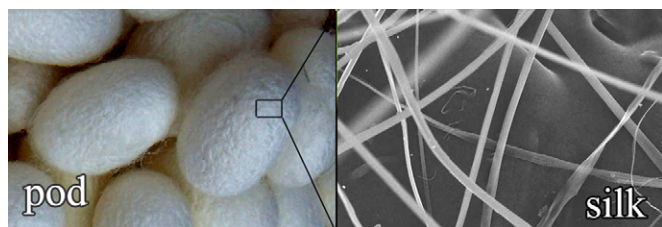


Fig. 1. Images of the pod and microstructure of the silk fibers.

## 2. Experimental

### 2.1. Sample preparation

Three groups of silk fibers were first immersed into three  $\text{Zr}(\text{NO}_3)_4$  solutions with different concentrations for 10 min. Their concentrations are 5%, 10%, and 15% with the solvent of water. Then, they were taken out and dried at 70 °C for 12 h. Finally, they were placed in an oxidation furnace and sintered at 800 °C for 2 h. Thus, the silk templates were removed and  $\text{ZrO}_2$  fibers were obtained.

### 2.2. Characterization

The microstructures of the materials were observed by using a scanning electronic microscope (SEM, JSM-6380, JEOL, Japan). The phases of the materials obtained in this study were identified by an X-ray diffractometer (XRD, Cu-K $\alpha$ , RigakuX 2038, Japan). The immersed silk and the original silk without immersing in solution were analyzed with a thermogravimetric analyzer (TG-DSC, SDT Q600, TA Instruments, US) in air. The temperature ranged from room temperature to 1000 °C. The heating rate was 20 °C/min. The Fourier transform infrared (FTIR) was carried out to the silk and the biomorphic  $\text{ZrO}_2$  (obtained by soaking in the 10% solution) by a spectrometer (Magna 560, Nicolet Instrument Corporation, US) in the wave number region 4000–500  $\text{cm}^{-1}$ . The samples of FTIR were made by mixing the materials with the KBr pellet, which was followed by pressing disk. To compare with the biomorphic fibers, the FTIR of the  $\text{ZrO}_2$  fiber made by the traditional sol–gel method was also measured.

### 2.3. Thermal conductivity

The thermal conductivities of the  $\text{ZrO}_2$  fibers (obtained by soaking in the 10% solution) were measured by the steady-state plate diathermometer. Its thermal conductivity at 100 °C was detected by J60 diathermometer (Shanghai Diathermometer Company, China) and those at 500 and 1000 °C were detected by PBD-02P diathermometer (Luoyang Institute of Refractories Research Co. Ltd., China). The apparent densities of the specimens are 0.096  $\text{g}/\text{cm}^3$ .

## 3. Results and discussion

### 3.1. Microstructures

Fig. 2 shows the full-scale photo of the  $\text{ZrO}_2$  derived from silk. It can be seen that this pile of material is composed of fibers, which indicates that the  $\text{ZrO}_2$  got the fibriform shape of silk.

Fig. 3a–c shows the microstructures of the  $\text{ZrO}_2$  fibers obtained by soaking in the solutions with different concentrations. These fibers retain the original fibrous silk morphology well, as compared with the microstructure of the silk in Fig. 1. The diameters of the  $\text{ZrO}_2$  fibers are in the range 10–15  $\mu\text{m}$ . The conformations of these  $\text{ZrO}_2$  fibers are controlled by nature, which is different from the traditional oxide fibers.

Fig. 4a and b shows the morphology of the silk fibers and the biomorphic  $\text{ZrO}_2$  fibers. The surface of the  $\text{ZrO}_2$  fiber is not as smooth as the silk. There are lots of scraggly rumples on its surface, which was formed during the decomposition of the  $\text{Zr}(\text{NO}_3)_4$ . It should be noted that many hollow  $\text{ZrO}_2$  fibers were found by the microscope. From the arrows in Fig. 4b, it can be seen obviously that the fibers are hollow. This is because that the  $\text{Zr}(\text{NO}_3)_4$  solute only covered the surfaces of the silk fibers after we immersed the silk into the solution and dried it. Then during heating, the solutes on the surfaces decomposed and turned into  $\text{ZrO}_2$  in situ, which was followed by removal of silk templates at higher temperature. Hence, after the silk is removed, the hollow fibers as shown in Fig. 4b can be obtained.

From Fig. 3, it can also be seen that the continuity of the fiber after soaking in the solution of higher concentration is better than that of lower concentration. The fibers in Fig. 3a and b have some ruptures and are a little shorter, but the fibers in Fig. 3c are longer. This is because that more  $\text{Zr}(\text{NO}_3)_4$  solute covered the surface of the silk fibers



Fig. 2. Full scale photo of biomorphic  $\text{ZrO}_2$ .

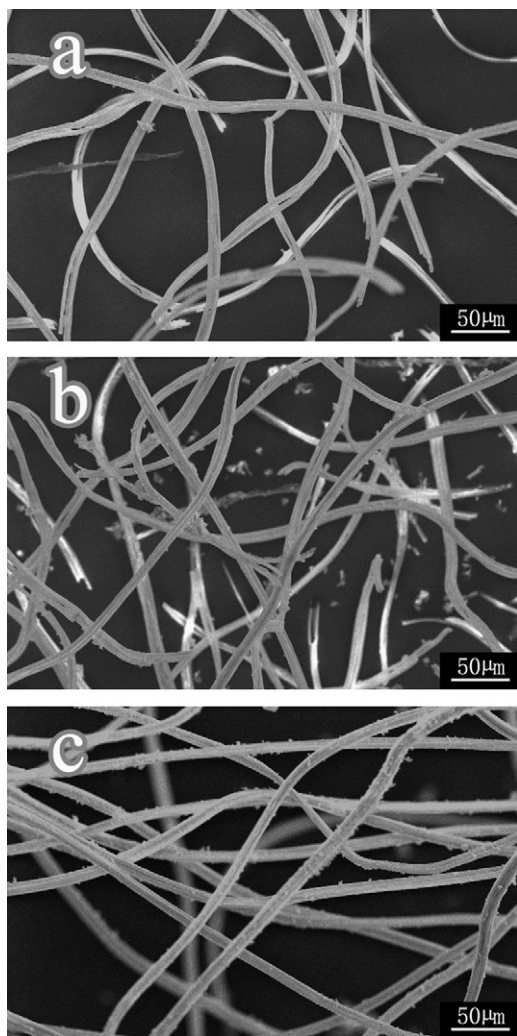


Fig. 3. SEM images of biomorphic  $\text{ZrO}_2$  fibers obtained by soaking in the solutions with different concentrations: (a) 5%, (b) 10%, and (c) 15%.

after soaking in the solution of higher concentration. Then, more  $\text{ZrO}_2$  formed and covered the silk after sintering. Thus, this  $\text{ZrO}_2$  fiber was stronger to keep the shape of silk more perfect when the silk-template was removed. Therefore, their continuity was improved with the increasing concentration.

### 3.2. XRD

The XRD pattern of the material derived from silk was shown in Fig. 5. The XRD pattern shows that the component of these biomorphic fibers is monoclinic  $\text{ZrO}_2$ . The average crystallite size of the biomorphic  $\text{ZrO}_2$  is 19.40 nm, which was calculated according to the Scherrer equation.

### 3.3. TG-DSC

Fig. 6a shows the TG-DSC thermogram of the original silk without immersing in the solution. There is a remarkable weight lost between 300 °C and 685 °C, with some

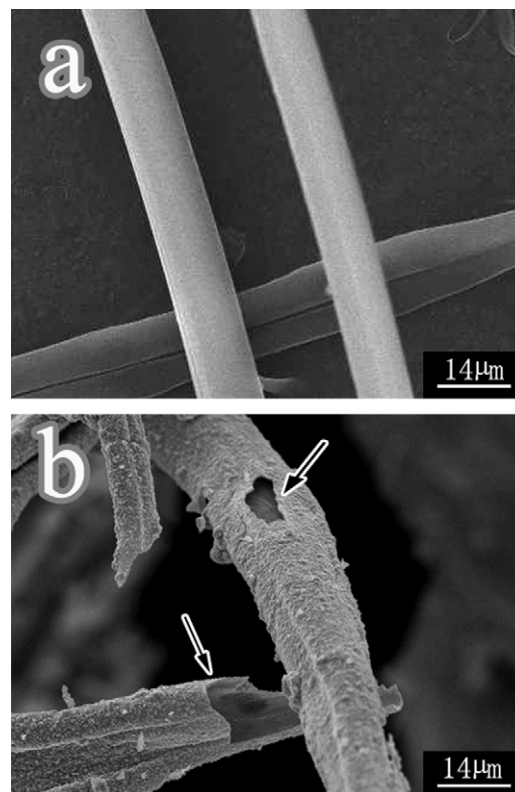


Fig. 4. Morphology of the silk fibers (a) and the hollow  $\text{ZrO}_2$  fibers (b).

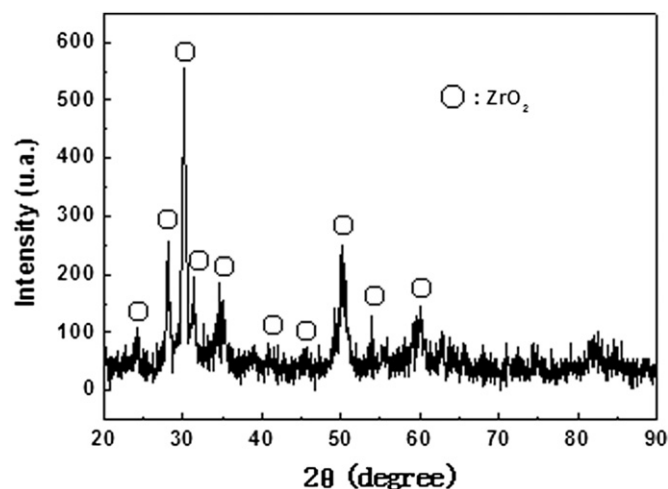


Fig. 5. XRD pattern of  $\text{ZrO}_2$  derived from silk.

exothermic peaks being found at 395, 594 and 677 °C. This is due to the decomposition and burning of the silk. Researchers found: silk is composed of two regions: the crystal region and the amorphous region [13]. Since the amorphous region is not as stable as the crystal region, the amorphous region can decompose and burn at lower temperature, as compared to the crystal region. Therefore, the exothermic peak at 395 °C is attributed to the burning of the amorphous region, and the peaks at 594 and 677 °C



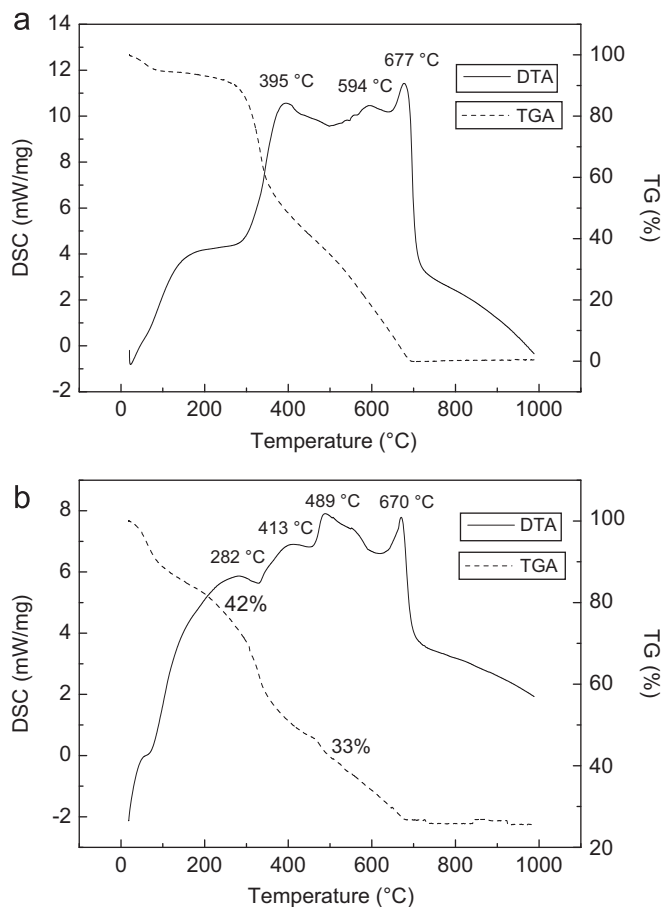


Fig. 6. TG-DSC thermograms of the original silk (a) and the immersed silk (b).

are attributed to the crystal region. Above 700 °C, the weight no longer goes down, but there are still no more than 0.5% residual materials. These remains may be the incomplete decomposed silk.

Fig. 6b shows the TG-DSC thermogram of the immersed samples below 1000 °C. As shown in this figure, there is an exothermic peak at 282 °C before the decomposition of the silk, corresponding to about 42% weight loss. It can be attributed to the decomposition of  $\text{Zr}(\text{NO}_3)_4$  to form  $\text{ZrO}_2$ . The decomposition of  $\text{Zr}(\text{NO}_3)_4$  was according to the following chemical reaction:  $\text{Zr}(\text{NO}_3)_4 \rightarrow \text{ZrO}_2 + \text{NO}_2 + \text{O}_2$ . There is another 33% weight loss between 340 and 680 °C, with three exothermic peaks being found at 413, 489, and 670 °C. This is due to the decomposition and burning of the silk. Compared to the original silk, the beginning of the decomposition and burning of the immersed silk was remitted to the higher temperature. It may be because of two reasons. One reason is that the silk here was covered with the insulating  $\text{ZrO}_2$  that could slow the heat transfer from outside to the silk inside. The other reason is that the oxygen was difficult to penetrate the covering  $\text{ZrO}_2$  so that the burning of the silk need higher temperature.

From the TG-DSC thermogram, it can be known that the fabrication process of these biomorphic fibers can be

separated into two steps: one is the formation of biomorphic  $\text{ZrO}_2$  fibers, and the other is the removal of their silk templates. Since the  $\text{ZrO}_2$  formed before the removal of the silk-template, the fibrous morphology of the silk could be retained to this  $\text{ZrO}_2$ .

### 3.4. FTIR spectra

Fig. 7 shows the contrast FTIR spectra of the silk, biomorphic  $\text{ZrO}_2$  (obtained by soaking in the 10% solution), and traditional  $\text{ZrO}_2$ . The absorption peaks for the silk sample at 3440, 2920 and 2850, 1660, 1590 and 1450, 1380, 1260, and 1090  $\text{cm}^{-1}$  correspond to the N–H in amine, C–H in methene, C=O in carboxyl and C=C in olefin, C=C in arene, C–H methyl, C–O in carboxyl, and C–N in amine. It is obvious that the absorption spectrum of the biomorphic  $\text{ZrO}_2$  fiber made from the silk is similar to that of the silk. Most of the peaks of the silk sample emerged in the spectrum of biomorphic  $\text{ZrO}_2$ , which indicates that the  $\text{ZrO}_2$  from silk inherited the good ability of absorbing infrared from the silk. This may be due to the incomplete decomposed silk included in the biomorphic fibers. However, these peaks did not emerge in the spectrum of the traditional  $\text{ZrO}_2$  fibers. There are little absorption peaks in its spectrum. It indicates that its ability of absorbing infrared is not as good as the biomorphic  $\text{ZrO}_2$  fibers.

### 3.5. Thermal conductivity

Fig. 8 shows the thermal conductivities of the biomorphic  $\text{ZrO}_2$  obtained by soaking in the 10% solution. Fig. 8 also shows the thermal conductivities of the traditional  $\text{ZrO}_2$  with the same apparent density ( $0.096 \text{ g/cm}^3$ ) as biomorphic  $\text{ZrO}_2$ , which were summarized in a review article by Hu et al. [14]. It can be seen that the thermal conductivities of the biomorphic  $\text{ZrO}_2$  are lower than that of the traditional  $\text{ZrO}_2$ , especially when the detecting temperature is 500 °C and 1000 °C. It indicates that this

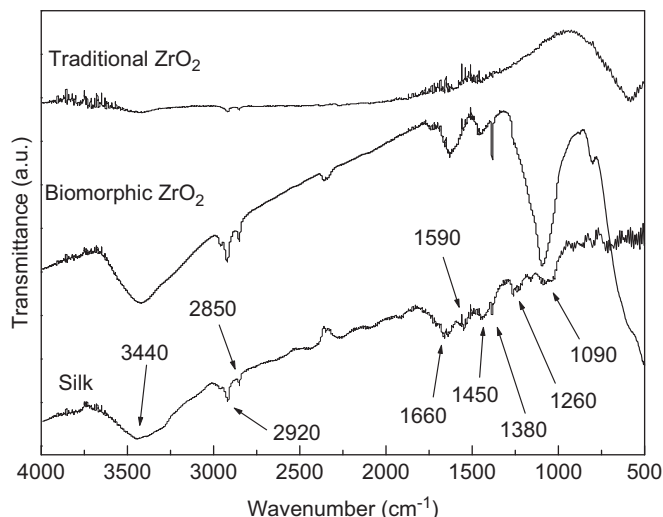


Fig. 7. FTIR spectra of the silk, biomorphic  $\text{ZrO}_2$  and traditional  $\text{ZrO}_2$ .

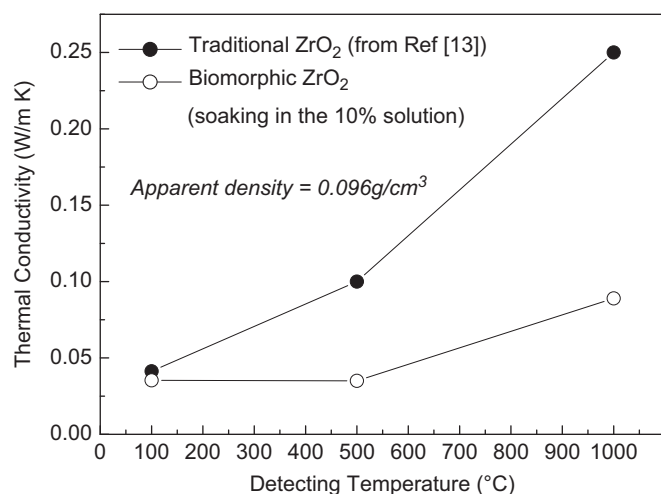


Fig. 8. Thermal conductivities of the biomorphic ZrO<sub>2</sub> and traditional ZrO<sub>2</sub>.

kind of ZrO<sub>2</sub> fibers has a much better heat-insulating property than the traditional ZrO<sub>2</sub> fibers. This may be due to two reasons.

One reason is that the hollow ZrO<sub>2</sub> fibers shown in Fig. 4b can prevent the convection of air and heat radiation more efficiently. Since the same apparent densities of these ZrO<sub>2</sub> fibers were used for the test of thermal conductivity, the contents of the air in the specimens were the same. If there were a large number of hollow fibers in the specimen, the air would be divided into more rooms and every room would have smaller volume. Thus, the convection of the air in the specimen would be restricted in each tiny room, and the convection in a wide range would become more difficult. At the same time, the more tiny rooms in the fibers can also cause the shorter mean free path of the photon, which made the heat radiation more difficult.

The other reason is that the incomplete decomposed silk made the biomorphic ZrO<sub>2</sub> fibers inherit the ability of absorbing infrared from the silk, as shown in Fig. 7. It is known that the silk has an excellent heat-insulating property. One of the reasons is that the silk can prevent the heat loss by absorbing the infrared that radiates inside the matter. Now this ability was left behind to the biomorphic fibers, which helped the biomorphic ZrO<sub>2</sub> fibers possess better thermal-insulating property than the traditional ZrO<sub>2</sub>.

In Fig. 8, the thermal conductivities of these fibers increase with the rising of the detecting temperature. However, the increment speed of the biomorphic ZrO<sub>2</sub> exhibits much slower than that of the traditional ZrO<sub>2</sub>. At low detecting temperature and small temperature gradient, the heat transfer in the fibers was caused mainly by heat transmittance. With the increasing of the detecting temperature and the temperature gradient, the heat radiation and convection of air would become the dominant means for heat transfer gradually. The hollow fibers could keep these two means not progressing too fast, so that the

biomorphic ZrO<sub>2</sub> had the lower increment speed of the thermal conductivity.

#### 4. Conclusions

This study provided a new method to fabricate high heat-insulating ZrO<sub>2</sub> fibers by using natural silk fibers as a bio-template. The processing principle of bio-template technologies was to treat the silk fibers with an inorganic solution and then to sinter at high temperature to form biomorphic ceramics. The ZrO<sub>2</sub> fibers retained the basic fibrous silk morphology well. Compared to the traditional ZrO<sub>2</sub> fibers, the biomorphic ZrO<sub>2</sub> has a better heat-insulating property because of its hollow structure and good ability of absorbing infrared that descended from the silk. The treatment by the solutions with different concentration can influence their crystal structures and has an effect on the continuity of ZrO<sub>2</sub>. The fabrication process of biomorphic ceramic included the formation of ZrO<sub>2</sub> and removal of their silk templates. Since it is different from the traditional fibers with their structures obtained artificially, this method of using bio-template could provide a new idea for designing of heat-insulating fiber.

#### Acknowledgments

The authors wish to express thanks to the National Natural Science Foundation of China (no. 51002077), Foundation of “Zijin Star” of “Excellence Program” of NJUST, and Science and Technology Development Program of NJUST (XKF09068).

#### References

- [1] A. Hartridge, M.D. Taylor, A.K. Bhattacharya, Synthesis and characterization of partially and fully stabilized zirconia fibers made from an inorganic precursor, *Journal of Materials Research* 16 (2001) 2384–2387.
- [2] G. Yu, L. Zhu, X. Wang, H. Che, G. Zhang, Z. Sun, H. Fan, X. Liu, D. Xu, Fabrication of zirconia mesoporous fibers by using polyorganozirconium compound as precursor, *Microporous and Mesoporous Materials* 119 (2009) 230–236.
- [3] P.K. Chakrabarty, M. Chatterjee, M.K. Naskar, B. Siladitya, D. Ganguli, Zirconia fiber mats prepared by a sol–gel spinning technique, *Journal of the European Ceramic Society* 21 (2001) 355–361.
- [4] R.C. Pullar, M.D. Taylor, A.K. Bhattacharya, The manufacture of partially-stabilized and fully-stabilized zirconia fibers blow spun from an alkoxide derived aqueous sol–gel precursor, *Journal of the European Ceramic Society* 21 (2001) 19–27.
- [5] J. Kim, S. Myoung, H. Kim, J. Lee, Y. Jung, C. Jo, Synthesis of SiC microtubes with radial morphology using biomorphic carbon template, *Materials Science and Engineering A* 434 (2006) 171–177.
- [6] P. Greil, E. Vogli, T. Fey, A. Bezold, N. Popovska, H. Gerhard, H. Sieber, Effect of microstructure on the fracture behavior of biomorphous silicon carbide ceramics, *Journal of the European Ceramic Society* 22 (2002) 2697–2707.
- [7] V. Pancholi, D. Mallick, C. Appa Rao, I. Samajdar, O.P. Chakrabarti, H.S. Maiti, R. Majumdar, Microstructural characterization using orientation imaging microscopy of cellular Si/SiC ceramics synthesized

- by replication of Indian dicotyledonous plants, *Journal of the European Ceramic Society* 27 (2007) 367–376.
- [8] G.J. Qiao, R. Ma, N. Cai, C.G. Zhang, Z.H. Jin, Mechanical properties and microstructure of Si/SiC materials derived from native wood, *Materials Science and Engineering A* 323 (2002) 301–305.
- [9] C. Zollfrank, R. Kladny, H. Sieber, P. Greil, Biomorphous SiOC/C-ceramic composites from chemically modified wood templates, *Journal of the European Ceramic Society* 24 (2004) 479–487.
- [10] R. Sun, L. Sun, Y. Chun, Q. Xu, H. Wu, Synthesizing nanocrystal-assembled mesoporous magnesium oxide using cotton fibers as exotemplate, *Microporous and Mesoporous Materials* 111 (2008) 314–322.
- [11] A. Zampieri, G.T.P. Mabande, T. Selvam, W. Schwieger, A. Rudolph, R. Hermann, H. Sieber, P. Greil, Biotemplating of luffa cylindrica sponges to self-supporting hierarchical zeolite macrostructures for bio-inspired structured catalytic reactors, *Materials Science and Engineering C* 26 (2006) 130–135.
- [12] T.C. Wang, T.X. Fan, D. Zhang, G.D. Zhang, Fabrication and wear behaviors of carbon/aluminum composites based on wood templates, *Carbon* 44 (2006) 900–906.
- [13] G. Liu, X. Wang, G. Hu, Thermal analysis and molecular structure of antheraea yamamai silk, *Journal of Zhejiang Institute of Silk Textiles* 10 (1) (1993) 1–5.
- [14] L. Hu, F. Gao, W. Chen,  $\text{ZrO}_2$  fiber and products, *Journal of Synthetic Crystals* 38 (1) (2009) 265–270.